ASME Open Journal of Engineering
Online journal at:
https://asmedigitalcollection.asme.org/openengineering

Pacific Ocean Windspeeds Prediction by Gaidai Multivariate Risks Evaluation Method, Utilizing Self-Deconvolution

Oleg Gaidai
College of Engineering Science and Technology,
Shanghai Ocean University,
Zhenjiang, Jiangsu 212003, China
e-mail: o_gaidai@just.edu.cn

The current study advances research on the consequences of global climate change by utilizing the novel Gaidai multivariate risks evaluation methodology to conduct spatiotemporal analysis of areal windspeeds. Multidimensional structural and environmental dynamic systems that have been either physically observed or numerically simulated over a representative time-lapse are particularly suitable for the Gaidai risks evaluation methodology. Current research also presents a novel non-parametric deconvolution extrapolation method. As this study has shown, given in situ environmental input, it is possible to accurately predict environmental system hazard risks, based even on a limited underlying dataset. Furthermore, because of their complex nonlinear cross-correlations between various environmental system-critical dimensions or components and large dimensionality, environmental dynamic systems are difficult to handle using traditional methods for evaluating risks. In the North Pacific, close to the Hawaiian Islands, NOAA buoys gathered raw in situ wind speed data, which has been utilized in the current study. Areal ocean wind speeds constitute quite a complex environmental dynamic system that is challenging to analyze because of its nonlinear, multidimensional, cross-correlated nature. Global warming had impacts on ocean windspeeds in the recent decade. Developing novel state-of-the-art environmental system risk evaluation methods is a principal component of modern offshore structural analysis in light of adverse weather. The advocated novel risk/hazard assessment approach may be used for resilient island cities design, especially those that are near ocean shore and hence exposed to extreme weather.
[DOI: 10.1115/1.4066682]

Keywords: climate, dynamic system, global warming, stochastics, windspeed, artificial intelligence, risk, risk analysis, risk and life cycle analysis, risk assessment, risk management, risk-based design, sustainable engineering

1 Introduction

High dimensionality of environmental systems with a large number of random variables impacting environmental system dynamics presents considerable challenges for the system's prognostics [1–5]. The reliability of complex environmental systems can be easily and precisely determined by using either a substantial amount of measurement data or direct large-scale MCS (Monte Carlo Simulations) [6–13]. Many complex environmental systems may be beyond the reach of computational or experimental resources. Driven by the aforementioned contention, writers propose an innovative approach to risk/hazard assessment for environmental systems, to minimize expenses related to computation or measurement [14]. Ocean wind speeds are usually modeled as a stochastic/random piecewise ergodic process. Figure 1 presents NOAA (i.e., National Oceanic and Atmospheric Administration) Blended Sea Winds global ocean windspeed dataset [15].

For practical renewable energy industrial purposes, capturing full wind energy resource potential, especially over offshore areas, is a challenging task. The role of renewable energy technologies in the framework of an integrated strategy to mitigate climate change is a topic of much interest to researchers these days. Most studies utilize generic EVT (i.e., Extreme Value Theory)-based parametric approaches [16,17], while this study advocates a more robust non-parametric statistical approach. As ocean wind and wave processes are closely inter-correlated, investigating the extreme occurrences of ocean waves has been attempted with some success, or freak waves, though this is outside the scope of this study, with PDF (i.e., Probability Density Function) reflecting physical system dynamics. For illustration, in Refs. [18,19], ocean waves deviate from linear theory, as the author has demonstrated. Similarly, in Refs. [20–24], authors have shown that Rayleigh-type PDF reflects hurricane data extreme events. Furthermore, it appears that the

Manuscript received June 9, 2024; final manuscript received September 16, 2024; published online October 11, 2024. Assoc. Editor: Kumaran Kannaiyan.

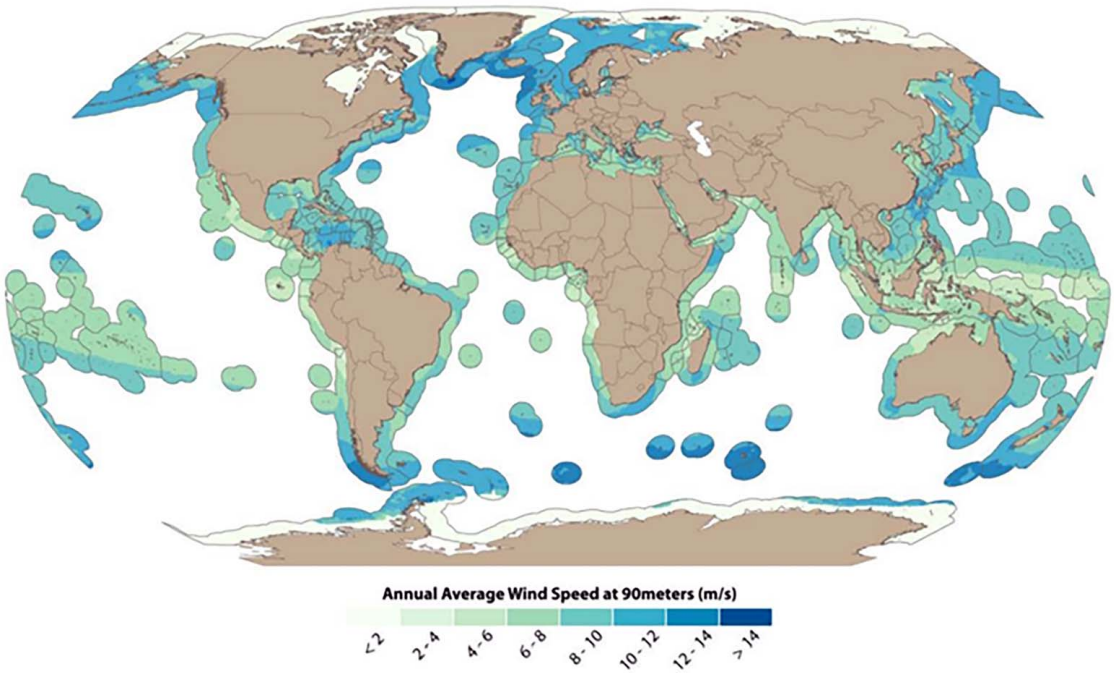

Fig. 1 An annual average windspeed map of Blended Sea Winds [15]

effects of spectrum bandwidth on the PDF of extreme waves vary depending on whether they occur in shallow or deep waters [25,26]. Moreover, experiments have shown a significant increase in the frequency of extreme waves due to ocean processes like Wave-current or shoaling systems that push wave trains out of balance [27–31]. It has recently been discovered that no known theoretical PDFs, whether grounded in physical principles or not, can account for extreme wave statistics in a variety of scenarios, and none can account for them universally like Gumbel can [32–44]. Note that the methodology introduced by authors here is nonparametric and thus does not rely on Gumbel, Weibull, Pareto, or any other GEV (i.e., Generalized Extreme Value) type of distribution. The worst wind-related damages in wind farms are often caused by extreme wind speed events. To prevent damage to wind turbines and minimize cut-out occurrences in these facilities, a precise assessment of the frequency and severity of extreme windspeed events has been recently conducted using generative data augmentation techniques [45]. Samples from representative known distributions are bootstrapped, and the validity of forecasts for high wind speeds at large mean recurrence intervals can be evaluated [46], where sub-asymptotic Gumbel-type distribution was employed, taking into account imperfect convergence to the proper asymptote, is compared to the conventional asymptotic GEV and GP (i.e., Generalized Pareto) distribution.

The capacity of the Gaidai risks evaluation methodology to analyze multidimensional spatiotemporal environmental systems with an almost infinite number of critical dimensions and components is a key innovation. Figure 2 provides a schematic flowchart of the Gaidai risks evaluation methodology for practical use in engineering applications – particularly during the design phase.

2 Multivariate Gaidai Risk Evaluation Method for Series-Type Systems

Assessing system reliability using traditional theoretical risk/hazard assessment methods is frequently a difficult undertaking. The majority of complex dynamic environmental systems have expenses associated with computation and experimentation that are typically prohibitive. To reduce the costs associated with measurement or computation, this paper proposes a novel way for risk/hazard assessment for dynamic environmental systems. Wind speed is generally considered to be a piecewise ergodic stochastic process that is homogenous and quasi-stationary. It is principal to analyze a dynamic MDOF (i.e., Multi-Degree-of-Freedom) system under in situ environmental stresses. A different approach would be to see the environmental system's operation as reliant on outside load factors, the temporal fluctuations of which can be represented as quasi-ergodic processes. The principal/key components $(X(t), Y(t), Z(t), \ldots)$ of the MDOF dynamic environmental system are those that have been measured or simulated during a specific representative period $(0, T)$. The global maxima of a one-dimensional (1D) environmental system-critical component over a representative time-lapse $(0, T)$ are represented here by the symbol, $X_T^{\max} = \max_{0 \le t \le T} X(t)$, $Y_T^{\max} = \max_{0 \le t \le T} Y(t)$, $Z_T^{\max} = \max_{0 \le t \le T} Z(t)$, … By "representative period" authors mean T value, large with

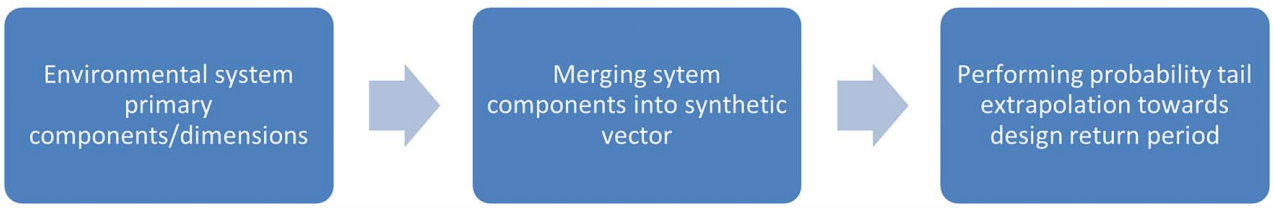

Fig. 2 Flowchart for Gaidai system multivariate reliability analysis

respect to autocorrelation and relaxation temporal scales of the dynamic environmental system. Let $X_1, \ldots, X_{N_X}$ stand for the temporally consequent local maxima of the environmental system component $X(t)$, recorded at discrete, monotonically increasing time-moments $t_1^X < \ldots < t_{N_X}^X$. In a similar way, the remaining system's primary 1D components $Y(t), Z(t), \ldots$ have local maxima $Y_1, \ldots, Y_{N_Y}$; $Z_1, \ldots, Z_{N_Z}, \ldots$ recorded in temporally increasing order. To keep things simple, we will assume that all local maxima in the environmental system are positive, and hence, all global maxima too. The objective now is to accurately estimate the probability/risk of environmental system failure/damage P_F

$$P_F \equiv 1 - P = \text{Prob}(X_T^{\max} > \eta_X \ \cup \ Y_T^{\max} > \eta_Y \ \cup \ Z_T^{\max} > \eta_Z \ \cup \ldots) \tag{1}$$

with

$$P = \iiint_{0,0,0,\ldots}^{(\eta_X,\eta_Y,\eta_Z,\ldots)} p_{X_T^{\max},Y_T^{\max},Z_T^{\max},\ldots}(x_T^{\max}, y_T^{\max}, z_T^{\max}, \ldots) dx_T^{\max} dy_T^{\max} dz_T^{\max} \ldots \tag{2}$$

Target survival (non-exceedance) probability/chances for critical/hazard levels of the main constituents of the environmental system, $\eta_X, \eta_Y, \eta_Z, \ldots$, with $p_{X_T^{\max},Y_T^{\max},Z_T^{\max}}, \ldots$ being the joint PDF of the environmental system's principal components global maxima, measured across $(0, T)$, and $\cup$ being the logical unity-operator «or». Due to joint PDF $p_{X_T^{\max},Y_T^{\max},Z_T^{\max}}, \ldots$ high dimensionality and underlying dataset limitations, it is not practical/feasible to evaluate it directly. The environmental system to be considered as failed/damaged when any of its principal components $X(t)$ had exceeded η_X; or $Y(t)$ had exceeded η_Y; or $Z(t)$ had exceeded η_Z; …, namely series-type system being assumed. Specific fixed/predefined levels of risk/failure/damage $\eta_X, \eta_Y, \eta_Z, \ldots$ for each system's principal 1D component: $X_{N_X}^{\max} = \max\{X_j; j = 1, \ldots, N_X\} = X_T^{\max}$, $Y_{N_Y}^{\max} = \max\{Y_j; j = 1, \ldots, N_Y\} = Y_T^{\max}$, $Z_{N_Z}^{\max} = \max\{Z_j; j = 1, \ldots, N_Z\} = Z_T^{\max}$, etc. Next, we will arrange the local maxima of the principal components of the environmental dynamic system, $[t_1^X < \ldots < t_{N_X}^X; t_1^Y < \ldots < t_{N_Y}^Y; t_1^Z < \ldots < t_{N_Z}^Z]$ in a monotonically increasing order, and combine them into a single 1D temporal vector $t_1 < \ldots < t_N$ with $t_N = \max\{t_{N_X}^X, t_{N_Y}^Y, t_{N_Z}^Z, \ldots\}$, $N \le N_X + N_Y + N_Z + \ldots$. The occurrence time of a local maxima of a critical component $X(t), Y(t), Z(t), \ldots$, will be represented by t_j. By means of temporally-concurrently screening for environmental system principal component's $X, Y, Z, \ldots$ local maxima, their exceedances of MDOF damage/limit/hazard vector $(\eta_X, \eta_Y, \eta_Z, \ldots)$ to be recorded. Environmental system's principal 1D components' local maxima had been merged into the synthetic temporally increasing system's vector $\vec{R} = (R_1, R_2, \ldots, R_N)$ in accordance with merged temporal system's vector $t_1 < \ldots < t_N$. The local maxima of the critical component of the system, which are connected to either component $X(t), Y(t), Z(t), \ldots$, were thus actually encountered by the component's local maxima R_j. At some point, the unified limit/hazard/damage system's vector $(\eta_1, \ldots, \eta_N)$ is added, with each system's critical component η_j being either $\eta_X, \eta_Y, \eta_Z, \ldots$, depending on whether of $X(t)$ or $Y(t)$, or $Z(t)$ …, corresponds to the local maximum of the current component's running index j. The scaling parameter $0 < \lambda \le 1$ may now be inserted in order to simultaneously decrease the limit values for all of the principal environmental dynamic system's components. Next, hazard/limit scaled limit vector $(\eta_1^\lambda, \ldots, \eta_N^\lambda)$ to be introduced, with η_j^λ being equal to either $\eta_X^\lambda, \eta_Y^\lambda, \eta_z^\lambda, \ldots$, or their maxima, in case local maxima from different components occur at the same time t_j, where $\eta_X^\lambda \equiv \lambda \cdot \eta_X$, $\eta_Y^\lambda \equiv \lambda \cdot \eta_Y$, $\eta_z^\lambda \equiv \lambda \cdot \eta_Z, \ldots$. Survival probability as $P(\lambda)$ of an environmental system becomes now smooth/differentiable C^1 function of λ, with $P \equiv P(1)$, and failure/damage probability $P_F \equiv 1 - P(1)$

$$\begin{aligned} P(\lambda) &= \text{Prob}\{R_N \le \eta_N^\lambda, \ldots, R_1 \le \eta_1^\lambda\} = \\ &= \text{Prob}\{R_N \le \eta_N^\lambda | R_{N-1} \le \eta_{N-1}^\lambda, \ldots, | R_1 \le \eta_1^\lambda\} \\ &\cdot \text{Prob}\{R_N \le \eta_N^\lambda | R_{N-1} \le \eta_{N-1}^\lambda, \ldots, | R_1 \le \eta_1^\lambda\} \\ &= \prod_{j=2}^{N} \text{Prob}\{R_j \le \eta_j^\lambda \mid R_{j-1} \le \eta_{j-1}^\lambda, \ldots, R_1 \le \eta_1^\lambda\} \cdot \text{Prob}(R_1 \le \eta_1^\lambda) \end{aligned} \tag{3}$$

The memory approximation that follows (conditioning memory depth k) may now be used since the dependence between neighboring R_j is not always negligible

$$\begin{aligned} &\text{Prob}\{R_j \le \eta_j^\lambda \mid R_{j-1} \le \eta_{j-1}^\lambda, \ .., R_1 \le \eta_1^\lambda\} \\ &\approx \text{Prob}\{R_j \le \eta_j^\lambda \mid R_{j-1} \le \eta_{j-1}^\lambda, \ .., R_{j-k} \le \eta_{j-k}^\lambda\} \end{aligned} \tag{4}$$

with $k < j \le N$. To put it simply, the idea behind this procedure is to keep an eye on each hazard or failure in chronological order of occurrence, preventing inter-correlated local exceedances from cascading or clustering. Probability functions $p_k(\lambda) \cdot \text{Prob}\{R_j > \eta_j^\lambda \mid R_{j-1} \le \eta_{j-1}^\lambda, \ R_{j-k+1} \le \eta_{j-k+1}^\lambda\}$ for $j \ge k$ is independent of j and solely reliant on the conditioning memory depth k, because the MDOF system was assumed to be jointly piecewise ergodic and thus jointly quasi-stationary. Currently, the likelihood of non-exceedance can be roughly expressed as

$$P_k(\lambda) \approx \exp(-N \cdot p_k(\lambda)), \ k \ge 1 \tag{5}$$

Since design damage/failure/hazard probability/risk being of the small order of magnitude $o(1)$, holding $N \gg k$, Eq. (5) follows from Eq. (1) by assuming $\text{Prob}(R_1 \le \eta_1^\lambda) \approx 1$. Convergence with regard to the conditioning parameter k is usual. Narrowband dynamic systems exhibit temporally successive/neighboring components as well as cascading/clustering hazards/failures/damages in significant environmental system's components. Due to the intrinsic interdependencies between nearby extreme events, local maxima appear as highly correlated groups or clusters of local maxima that are stored in the synthetic vector $\vec{R} = (R_1, R_2, \ldots, R_N)$ of the assembled system [47–55]. The system's vector $\vec{R}$ is made up of N, the total number of local maxima of the system's critical component (Fig. 3) [56–60].

Using a running index of j, the unified system limit/hazard vector $(\eta_1, \ldots, \eta_N)$ has each component η_j equal to either $\eta_X, \eta_Y, \eta_Z, \ldots,$, depending on which principal component, $X(t), Y(t), Z(t), \ldots,$ corresponds to the current local maxima.

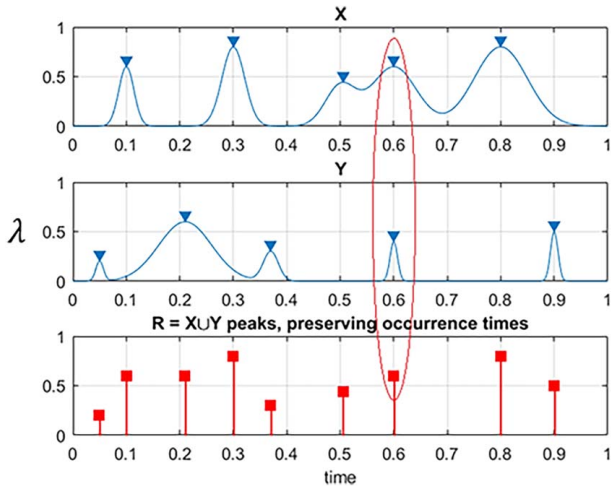

Fig. 3 Illustration of two system's components *X*, *Y*, being combined into 1D synthetic system vector *R*. Ellipse marks the case of simultaneous maxima occurrence for two different system's components.

2.1 Self-Deconvolution Extrapolation Scheme. Assume that a quasi-stationary stochastic/random process $X(t)$ may be expressed as the sum of two distinct quasi-stationary processes, $X_1(t)$ and $X_2(t)$, and that $X(t)$ being either directly measured or MC (Monte Carlo) simulated over a typical time-lapse, $0 \le t \le T$

$$X(t) = X_1(t) + X_2(t) \tag{6}$$

This work aims to introduce a flexible non-parametric extrapolation technique that may be used to forecast extreme values for a wide range of complex environmental dynamic systems. For the stochastic process of interest $X(t)$, there are two ways to generate the target marginal PDF p_X:

(A) straightforward extracting p_X^A from the underlying dataset, namely from underlying time series $X(t)$
(B) After the PDFs from each of the principal stochastic process components $X_1(t)$, $X_2(t)$, or p_{X_1}, p_{X_2} are extracted independently, the convolution $p_X^B = \text{conv}(p_{X_1}, p_{X_2})$ is applied.

where p_X^A and p_X^B are therefore approximations of the target PDF p_X. While method (B) may produce more accurate PDF p_X estimations, Method (A) is far simpler to use. The convolution scenario has the benefit of allowing empirical PDF p_X^A to be extrapolated (directly extracted from method B) without assuming any particular extrapolation-functional group or class (like GEV), which is required to extrapolate PDF tail towards the low probability levels of interest (long return periods) of the design. The majority of extrapolation techniques employed in modern engineering practice require a specific extrapolation-functional class [56–58,61]. Here are a few of popular parametric extrapolation methods: POT (i.e., Peaks Over the Threshold), Gumbel fit, and Generalized Pareto-based PDF [59,60]. In the current study, we will consider only self-convolution case: $p_{X_1} = p_{X_2}$, searching for two IID. (Independent Identically Distributed) process parts/components, $X_1(t)$, $X_2(t)$. Following (A), the current objective is to assess the component's PDF p_{X_1}

$$p_X = \text{conv}(p_{X_1}, p_{X_1}) \tag{7}$$

As such, only the self-deconvolution scenario will be examined in the ensuing investigation. The region where vectors $\boldsymbol{u}$ and $\boldsymbol{v}$ overlap is known as a convolution of two vectors. Because of this, convolution and polynomial multiplication in which the coefficients are parts of $\boldsymbol{u}$ and $\boldsymbol{v}$ have algebraic similarities. Let denote $m = \text{length}(\boldsymbol{u})$ and $n = \text{length}(\boldsymbol{v})$; then, $\boldsymbol{w}$ is a vector with length $m + n - 1$ with kth element

$$w(k) = \sum_{j=1}^{m} u(j)v(k - j + 1) \tag{8}$$

Note that for self-deconvolution case $\boldsymbol{u} = \boldsymbol{v}$ and $m = n$. The vector $\boldsymbol{w}$ is projected and stretched to a length twice that of the original PDF support domain. To sum up, the PDF support length p_X has increased twice, $(2n - 1) \cdot \Delta x \approx 2n \cdot \Delta x = 2X_L$, in comparison to the starting length $n \cdot \Delta x = X_L$. Since empirical PDFs are not smooth in the tail, a smoothing tail procedure is required. Næss-Gaidai (NG or modified four-parameter Weibull) approach has been also used here, since PDF tails resemble $\exp\{-(ax+b)^c + d\}$ at $x \ge x_0$, where a, b, c, d being four optimized parameters. The proposed approach may also make use of other extrapolation approaches; however, doing so would include some biases and assumptions. To get the PDF tail, deconvolution extrapolation does not have to adhere to any specific extrapolation-functional group or class. Given the CDF (i.e., Cumulative Distribution Function), it is more principal to assess the likelihood of exceedance or $\overline{\text{CDF}} = 1 - \text{CDF}$, than the marginal PDF/$\overline{\text{CDF}}$.

3 Results

In order to illustrate the efficacy of the Gaidai risks evaluation approach in the North Pacific, this section makes use of the 10-min average wind speed measurements in the m/s dataset from the NOAA buoy, close to the Hawaii islands. Wind speed dynamics is widely acknowledged to be a multidimensional, highly nonlinear, cross-correlated dynamic system that can be challenging to analyze. Environmental system risk/hazard assessment techniques are also principal for marine structures that operate in a specific offshore region of interest and are occasionally exposed to severe offshore weather.

Considering three NOAA offshore wind measurement sites, (1) Station 51101 (LLNR 28006.3)—NW of Hawaii; (2) Station 51002—SW of Hawaii; Station (3) 51000 – northern (N) Hawaii,

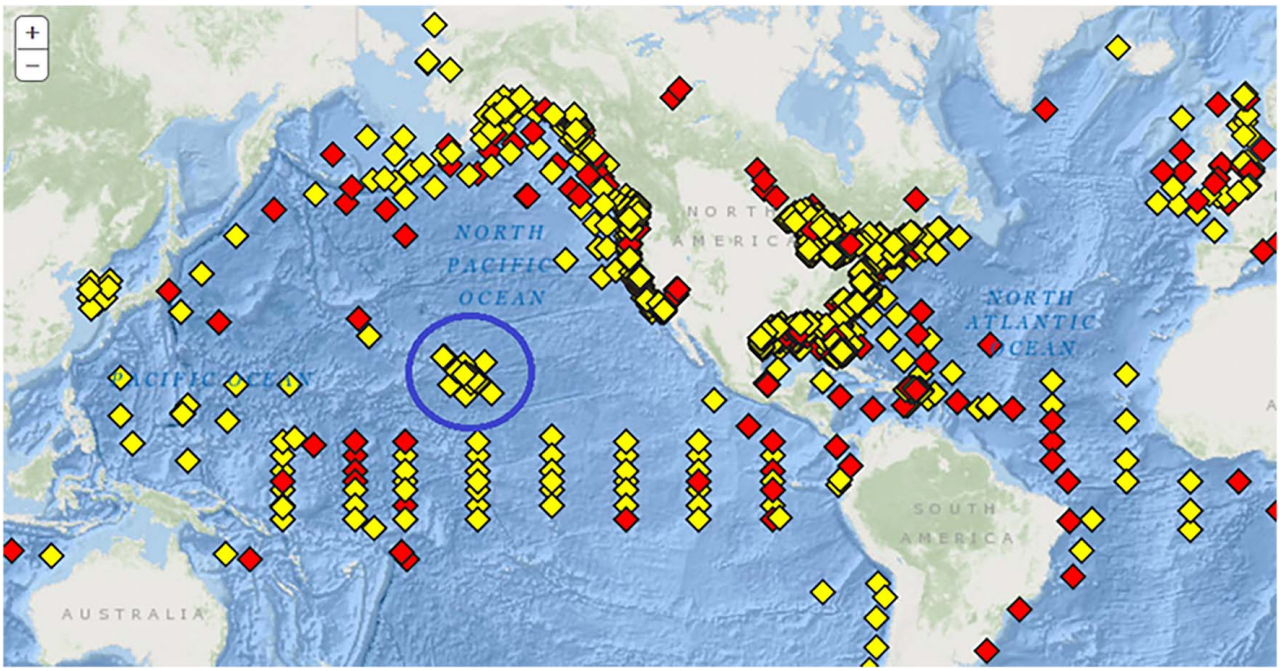

Fig. 4 Windspeed measurements locations near Hawaii islands, according to NOAA; circle marks the area of interest

had been chosen in the current study, its respective measured 10-min average windspeed values in m/s have been chosen as three environmental system's critical components (or dimensions) X, Y, Z thus constituting an example of 3D (i.e., three dimensional) environmental system. Critical limits either η_X, η_Y, or η_Z for the 1D system's critical/key components have been set equal to the whole analyzed dataset's maximum windspeeds, during a decade observation period between years 2009–2018, monitored synchronously for all three chosen windspeed measurement buoy's locations. Figure 4 provides North Pacific NOAA buoy locations [34], and the Area of interest indicated by a blue circle.

Figure 5 shows the NOAA data buoy, comprising sensors that track and gather information on oceanic and atmospheric conditions. The information is then converted into an electrical signal, which is either recorded in the onboard data unit or transmitted to land. The parameters/sensors feature of the 3-meter NOAA buoy are as follows:

- Site elevation: MSL (i.e., Mean Sea Level);
- Height of air temperature: 3.4 meters above MSL;
- The height of the anemometer is 3.8 meters above MSL;
- Barometer elevation: 2.4 meters above MSL;
- Sea temperature: 2 meters below MSL;
- Ocean depth: 2 km.

To integrate the three measured time series, X, Y, Z the scaling that follows was carried out in compliance with Eq. (2). This led to the key components of all three environmental systems being non-dimensional and having equal failure, danger, and damage limitations of 1. After that, all of the local maxima from the three measured time series were merged into one synthetic time series by sorting all of the sets $\max\{X_j, Y_j, Z_j\}$ according to the chronologically increasing occurrences of occurrence of these system-critical component's local maxima. This was done by retaining the local maxima in the temporally rising order: $\vec{R} = (\max\{X_1, Y_1, Z_1\}, \ldots, \max\{X_N, Y_N, Z_N\})$. A non-dimensional example of an assembled/synthetic vector $\vec{R}$ is shown in Fig. 6. This dataset is an assembly of the raw daily greatest highest daily hindcast wind speed dataset's local maxima.

Fig. 5 NOAA Buoy [34]

Using the PDF tail, the target failure/damage probability/risk level was extrapolated to a 100-year return period. It should be highlighted that a synthetic vector $\vec{R}$ has no specific physical importance on its own because it is composed of completely different primary components of the environmental system. The "shorter" data record was created by taking the 10th data point from the «full/longer» wind speed dataset. The "shorter" dataset's f_{X_1} PDF tail is shown in Fig. 7(*a*). It was created by deconvolution and then linearly extrapolated in the PDF's terminal tail section to encompass the X_1 range that corresponds to the "full/longer" dataset. The final unscaled results by the Gaidai hazards assessment approach are shown in Fig. 7(*b*); this comprises the deconvolution-based extrapolation of the «shorter» decimal log scale f_X tail and the PDF tail and NG extrapolation of the «full/longer» data.

It can be seen that the NG prediction and the Gaidai risk assessment approach agree fairly well. Figure 7(*b*) illustrates how well the Gaidai risks assessment approach works, despite being based on a "shorter" dataset and producing a distribution that is fairly similar to that of datasets based on a "full/longer" dataset. Extrapolation results, based on the «shorter» dataset, have been found to differ less than 10% from those based on the «full/longer» dataset, for 100-year return period of interest [12]. Note that a 10% accuracy deviation is well accepted for practical engineering reliability/design purposes. Figure 7(*b*) presents extrapolations towards a 100-year return period, which corresponds to $\lambda = 1$, with $\lambda = 0.05$ being the extrapolation cut-on value. $p(\lambda)$ is directly related to the desired failure/hazard probability/risk $1 - P$ from Eq. (1) after using Eq. (5). Therefore, $1 - P \approx 1 - P_k(1)$ may be evaluated by Eq. (5) environmental system failure/hazard/damage probability/risk. It should be emphasized that the parameter N in Eq. (5) denotes the total number of local maxima in the unified synthetic vector $\vec{R}$. Convergence of the conditioning memory depth parameter $k = 3$ is convergent. Note that the above-described novel methodology possesses clear advantages of being able to utilize available MC simulated/measured multidimensional datasets efficiently, due to its capacity to handle the multidimensionality of environmental systems and its ability to carry out precise extrapolation from a relatively small underlying dataset. Non-stationary systems with a distinct underlying trend can benefit from the application of the Gaidai hazards assessment approach. The measurements can be brought to a quasi-stationary state by subtracting the underlying pattern, if one is aware of it. If not, appropriate trend analysis would be required in addition to the Gaidai technique for evaluating risks [62–77]. The second-order difference plot is derived from the Poincare plot

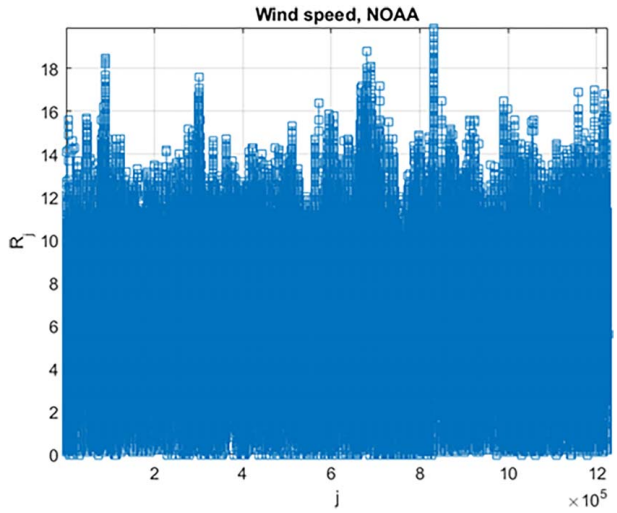

Fig. 6 Dimensional assembled synthetic vector $\vec{R}$, composed of daily 10-min average windspeeds values in m/s

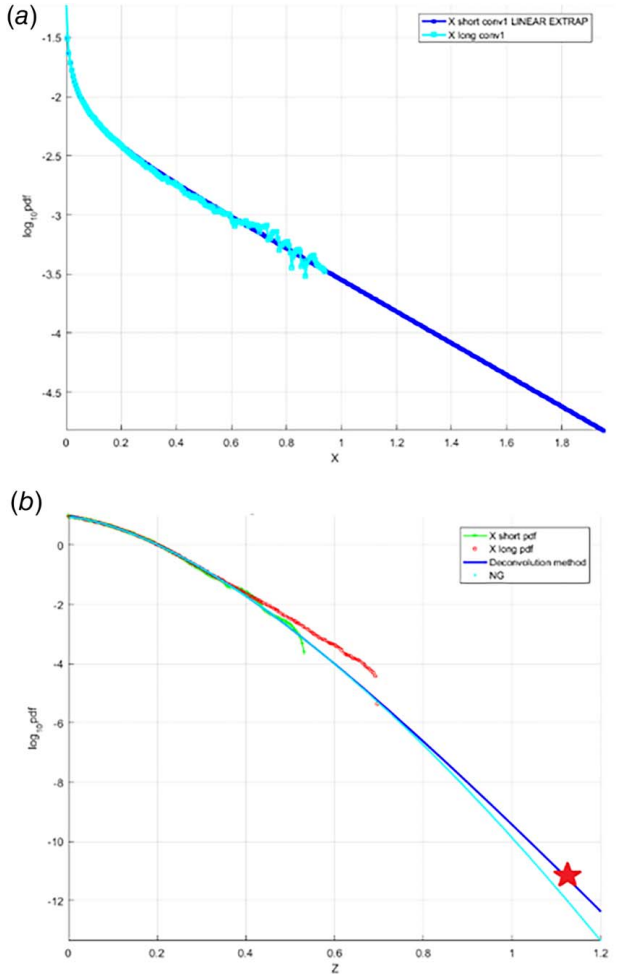

Fig. 7 Wind speed extrapolation from raw data. (*a*) Scaled f_{X_1} tail, linearly extrapolated, on the decimal log scale for the «shorter» dataset. (*b*) The unscaled raw tail of the «shorter» data f_X on the decimal log scale, along with the «full/longer» entire dataset and the NG extrapolation, are extrapolated using the deconvolution method. The target 100-year return period level is indicated by a star.

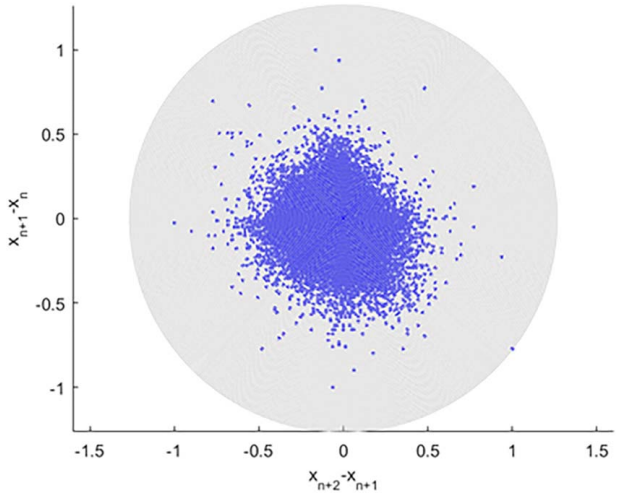

Fig. 8 Wind speed Second-order SODP plot exhibiting square-like pattern/shape

(SODP). Within the underlying dataset, SODP tracks statistical trends of sequential differences.

Figure 8 presents a second-order SODP plot, which may be used for identification of the underlying dataset's patterns, and comparison with other pertinent datasets, such as entropy AI (i.e., Artificial Intelligence) recognition techniques [78]. Extreme windspeed at an offshore location was predicted using the MCS and MCP (i.e., Measure–Correlate–Predict) approach. Extreme windspeeds computed from the combined PDF acquired by the MCP and MCS approaches agree well with the actual in situ data in a nation with a mixed environment like Japan, when compared to the combined PDF derived by the MCP method alone [79]. As a result, it was shown that in mixed climates, the 50-year recurrent windspeed error of the MCS technique is substantially smaller than that of the MCP approach. Figures 6 and 7 represent the application of the Gaidai risks evaluation method to the raw underlying dataset, i.e., to the unfiltered measured dataset. Note that various extrapolation methods can be plugged into the Gaidai risks evaluation method, hence not limited only to the four-parameter Weibull-type or Gumbel-type methods [80–85]. Recently novel deconvolution extrapolation method has been developed by authors and has been described in the previous section. The deconvolution method's major advantage is the fact that it is not parametric, hence extrapolation is less prone to optimization errors. Note that the advocated multimodal Gaidai risks evaluation method is mathematically exact; hence, inaccuracies may arise either from the underlying dataset itself or from the chosen extrapolation method [86–91].

4 Discussion

Presented case study, primarily aimed to further benchmark state-of-the-art Gaidai multivariate reliability methodology, along with novel deconvolution extrapolation scheme. Existing reliability techniques, when applied to raw measured time series, are not always applicable to environmental systems with spatiotemporal complexity and nonlinear cross-correlations between numerous principal components. The primary benefit of the suggested methodology is its capacity to evaluate high-dimensional nonlinear environmental dynamic system's reliability. Presented study analyzed 10-min average windspeeds, measured by NOAA buoys around the Hawaiian Islands in the North Pacific, during the decade 2009–2018. The probability of extreme events with a 100-year return period had been forecasted. A detailed description of the theoretical foundation of the suggested Gaidai hazards assessment technique has been provided. Because environmental systems are highly dimensional and complex, there is a constant need to create precise, inventive, and dependable solutions that make efficient use of the limited number of underlying datasets that are now available [92–99].

Gaidai risks evaluation methodology, presented in this work, has already been used in a range of practical applications, however only for the system's one-dimensional components, yielding on average accurate predictions. The main goal of this study was to develop and enhance a multidimensional, flexible, and dependable methodology for evaluating risks. The advocated methodology may be applied to a variety of environmental nonlinear dynamic system reliability evaluations. Predicted values have been cross-validated versus the alternative extrapolation method, and reasonable agreement has been reported. A primary constraint of the recommended methodology was the joint quasi-stationarity of the system. If there is an underlying trend in the environmental system, it must be identified first.

Author Contribution Statement

All authors contributed equally.

Conflict of Interest

There are no conflicts of interest. This article does not include research in which human participants were involved. Informed consent is not applicable. This article does not include any research in which animal participants were involved.

Data Availability Statement

The datasets generated and supporting the findings of this article are obtainable from the corresponding author upon reasonable request.

Abbreviations

CI	=	confidence interval
CDF	=	cumulative distribution function
EVT	=	extreme value theory
GEV	=	generalized extreme value (theory)
MDOF	=	multi-degree-of-freedom (system)
MUR	=	mean up-crossing rate
NAG	=	Numerical Algorithm Group
NG	=	Næss-Gaidai extrapolation scheme (modified four-parameter Weibull)
NOAA	=	National Oceanic and Atmospheric Administration (USA)
MC	=	Monte Carlo (method)
MCS	=	Monte Carlo Simulations
PDF	=	probability density function
POT	=	peaks over the threshold

References

[1] Christou, M., and Ewans, K., 2014, "Field Measurements of Rogue Water Waves," J. Phys. Oceanogr., **44**(9), pp. 2317–2335.
[2] Doeleman, M. W., 2021, "Rogue Waves in the Dutch North Sea," Master's thesis, TU Delft, Delft, The Netherlands.
[3] Ducrozet, G., Abdolahpour, M., Nelli, F., and Toffoli, A., 2021, "Predicting the Occurrence of Rogue Waves in the Presence of Opposing Currents With a High-Order Spectral Method," Phys. Rev. Fluids, **6**(6), p. 064803.
[4] Forristall, G., 1978, "On the Distributions of Wave Heights in a Storm," J. Geophys. Res., **83**(C5), pp. 2353–2358.
[5] Gaidai, O., Xu, X., Wang, J., Ye, R., Cheng, Y., and Karpa, O., 2020, "SEM-REV Offshore Energy Site Wind-Wave Bivariate Statistics by Hindcast," Renewable Energy, **156**, pp. 689–695.
[6] Gaidai, O., Yan, P., and Xing, Y., 2023, "Future World Cancer Death Rate Prediction," Sci. Rep., **13**(1), p. 303.
[7] Gaidai, O., Xu, J., Hu, Q., Xing, Y., and Zhang, F., 2022, "Offshore Tethered Platform Springing Response Statistics," Sci. Rep., **12**(1), p. 21182.
[8] Gaidai, O., Xing, Y., and Xu, X., 2023, "Novel Methods for Coupled Prediction of Extreme Windspeeds and Wave Heights," Sci. Rep., **13**(1), p. 1119.
[9] Gaidai, O., Cao, Y., Xing, Y., and Wang, J., 2023, "Piezoelectric Energy Harvester Response Statistics," Micromachines, **14**(2), p. 271.
[10] Gaidai, O., Cao, Y., and Loginov, S., 2023, "Global Cardiovascular Diseases Death Rate Prediction," Curr. Probl. Cardiol., **485**(5), p. 101622.
[11] Rice, S. O., 1944, "Mathematical Analysis of Random Noise," Bell Syst. Tech. J., **23**(3), pp. 282–332.
[12] Madsen, H. O., Krenk, S., and Lind, N. C., 1986, *Methods of Structural Safety*, Prentice-Hall Inc, Englewood Cliffs.
[13] Ditlevsen, O., and Madsen, H. O., 1996, *Structural Reliability Methods*, John Wiley & Sons, Inc, Chichester (UK).
[14] Gaidai, O., Wang, F., Wu, Y., Xing, Y., Rivera Medina, A., and Wang, J., 2022, "Offshore Renewable Energy Site Correlated Wind-Wave Statistics," Probabilistic Eng. Mech., **68**, p. 103207.
[15] Gaidai, O., Cao, Y., Zhu, Y., Zhang, F., and Li, H., 2024, "Multivariate Risk Assessment for Offshore Jacket Platforms by Gaidai Reliability Method," J. Marine. Sci. Appl.
[16] Glukhovskii, B., 1966, *Investigation of Sea Wind Waves (in Russian)*, Gidrometeoizdat, Moscow, Russia.
[17] Gaidai, O., Liu, Z., Cao, Y., et al., 2024, "Extreme Wave Parameters Based on Continental Shelf Storm Wave Records," J. Vib. Control, pp. 151–170.
[18] Tayfun, M. A., 1980, "Narrow-Band Nonlinear Sea Waves," J. Geophys. Res., **85**(C3), pp. 1548–1552.
[19] Tayfun, M. A., and Fedele, F., 2007, "Wave-Height Distributions and Nonlinear Effects," Ocean Eng., **34**(11–12), pp. 1631–1649.
[20] Jahns, H., and Wheeler, J., 1973, "Long-Term Wave Probabilities Based on Hindcasting of Severe Storms," J. Petrol. Technol., **25**(4), pp. 473–486.
[21] Kinsman, B., 1960, Surface Waves at Short Fetches and Low Windspeed – a Field Study. Chesapeake Bay Institute Technical Report.
[22] Li, Y., Draycott, S., Adcock, T. A., and Van Den Bremer, T., 2021, "Surface Wavepackets Subject to an Abrupt Depth Change. Part 2: Experimental Analysis," J. Fluid Mech., **915**, p. A72.
[23] Li, Y., Draycott, S., Zheng, Y., Lin, Z., Adcock, T., and Van Den Bremer, T., 2021, "Why Rogue Waves Occur Atop Abrupt Depth Transitions," J. Fluid Mech., **919**, p. R5.
[24] Li, Y., Zheng, Y., Lin, Z., Adcock, T. A., and Van Den Bremer, T., 2021, "Surface Wavepackets Subject to an Abrupt Depth Change. Part 1: Second-Order Theory," J. Fluid Mech., **915**, p. A71.
[25] Longuet-Higgins, M., 1952, "On the Statistical Distribution of the Heights of Sea Waves," J. Mar. Res., **11**, pp. 245–265.
[26] Longuet-Higgins, M. S., 1980, "On the Distribution of the Heights of Sea Waves: Some Effects of Nonlinearity and Finite Band Width," J. Geophys. Res., **85**(C3), pp. 1519–1523.
[27] Majda, A., Moore, M., and Qi, D., 2019, "Statistical Dynamical Model to Predict Extreme Events and Anomalous Features in Shallow Water Waves With Abrupt Depth Change," Proc. Natl. Acad. Sci. U. S. A., **116**(10), pp. 3982–3987.
[28] Mendes, S., and Kasparian, J., 2022, "Saturation of Rogue Wave Amplification Over Steep Shoals," Physical Review E. Accepted for publication. https://journals.aps.org/pre/accepted/a2077KaaI041ec0626a21bd0ec4388c81ed896128. arXiv: physics.flu-dyn/2207.13869.
[29] Mendes, S., and Scotti, A., 2021, "The Rayleigh-Haring-Tayfun Distribution of Wave Heights in Deep Water," Appl. Ocean Res., **113**, p. 102739.
[30] Mendes, S., Scotti, A., Brunetti, M., and Kasparian, J., 2022, "Non-Homogeneous Model of Rogue Wave Probability Evolution Over a Shoal," J. Fluid Mech., **939**, p. A25.
[31] Mendes, S., Scotti, A., and Stansell, P., 2021, "On the Physical Constraints for the Exceeding Probability of Deep-Water Rogue Waves," Appl. Ocean Res., **108**, p. 102402.
[32] Miles, J., 1957, "On the Generation of Surface Waves by Shear Flows," J. Fluid Mech., **3**(2), pp. 185–204.
[33] Moore, N., Bolles, C., Majda, A., and Qi, D., 2020, "Anomalous Waves Triggered by Abrupt Depth Changes: Laboratory Experiments and Truncated KDV Statistical Mechanics," J. Nonlinear Sci., **30**(6), pp. 3235–3263.
[34] National Oceanic and Atmospheric Administration. https://www.ndbc.noaa.gov
[35] Phillips, O., 1957, "On the Generation of Waves by Turbulent Wind," J. Fluid Mech., **2**(5), pp. 417–445.
[36] Phillips, O., 1958, "The Equilibrium Range in the Spectrum of Wind-Generated Waves," J. Fluid Mech., **4**(4), pp. 426–434.
[37] Phillips, O., 1985, "Spectral and Statistical Properties of the Equilibrium Range in Wind-Generated Gravity Waves," J. Fluid Mech., **156**(1), pp. 505–531.
[38] Pierson, W. J., and Marks, W., 1952, "The Power Spectrum Analysis of Ocean-Wave Records," Trans. Am. Geophys. Union, **33**(6), pp. 834–844.
[39] Pierson, W. J., and Moskowitz, L., 1964, "A Proposed Spectral Form for Fully Developed Wind Seas Based on the Similarity Theory of s. a. Kitaigorodskii," J. Geophys. Res., **69**(24), pp. 5181–5190.
[40] Stansell, P., 2004, "Distribution of Freak Wave Heights Measured in the North Sea," Appl. Ocean Res., **26**(1–2), pp. 35–48.
[41] Toffoli, A., Waseda, T., Houtani, H., Cavaleri, L., Greaves, D., and Onorato, M., 2015, "Rogue Waves in Opposing Currents: An Experimental Study on Deterministic and Stochastic Wave Trains," J. Fluid Mech., **769**, pp. 277–297.
[42] Trulsen, K., Raustøl, A., Jorde, S., and Rye, L., 2020, "Extreme Wave Statistics of Long-Crested Irregular Waves Over a Shoal," J. Fluid Mech., **882**, p. R2.
[43] Trulsen, K., Zeng, H., and Gramstad, O., 2012, "Laboratory Evidence of Freak Waves Provoked by Non-Uniform Bathymetry," Phys. Fluids, **24**(9), p. 097101.
[44] Wu, Y., Randell, D., Christou, M., Ewans, K., and Jonathan, P., 2016, "On the Distribution of Wave Height in Shallow Water," Coastal Eng., **111**, pp. 39–49.
[45] Vega-Bayo, M., Pérez-Aracil, J., Prieto-Godino, L., and Salcedo-Sanz, S., 2023, "Improving the Prediction of Extreme Wind Speed Events With Generative Data Augmentation Techniques," Renewable Energy, **221**, p. 119769.
[46] Cook, N. J., 2023, "Reliability of Extreme Wind Speeds Predicted by Extreme-Value Analysis," Meteorology, **2**(3), pp. 344–367.
[47] Gaidai, O., and Xing, Y., 2022, "A Novel Bio-System Reliability Approach for Multi-State COVID-19 Epidemic Forecast," Eng. Sci., **21**(18), p. 797.
[48] Gaidai, O., Xu, J., Yan, P., Xing, Y., Zhang, F., and Wu, Y., 2022, "Novel Methods for Windspeeds Prediction Across Multiple Locations," Sci. Rep., **12**(1), p. 19614.
[49] Gaidai, O., and Xing, Y., 2022, "Novel Reliability Method Validation for Offshore Structural Dynamic Response," Ocean Eng., **266**(5), p. 113016.
[50] Gaidai, O., Wu, Y., Yegorov, I., Alevras, P., Wang, J., and Yurchenko, D., 2022, "Improving Performance of a Nonlinear Absorber Applied to a Variable Length Pendulum Using Surrogate Optimization," J. Vib. Control, **30**(1–2), pp. 156–168.
[51] Gaidai, O., Wang, K., Wang, F., Xing, Y., and Yan, P., 2022, "Cargo Ship Aft Panel Stresses Prediction by Deconvolution," Mar. struct., **88**, p. 103359.
[52] Gaidai, O., Xu, J., Xing, Y., Hu, Q., Storhaug, G., Xu, X., and Sun, J., 2022, "Cargo Vessel Coupled Deck Panel Stresses Reliability Study," Ocean Eng., **268**, p. 113318.
[53] Gaidai, O., and Xing, Y., 2022, "A Novel Multi Regional Reliability Method for COVID-19 Death Forecast," Eng. Sci., **21**(16), p. 799.
[54] Gaidai, O., Yan, P., Xing, Y., Xu, J., Zhang, F., and Wu, Y., 2023, "Oil Tanker Under Ice Loadings," Sci. Rep., **13**(1), p. 8670.
[55] Gaidai, O., Xing, Y., Xu, J., and Balakrishna, R., 2023, "Gaidai-Xing Reliability Method Validation for 10-MW Floating Wind Turbines," Sci. Rep., **13**(1), p. 8691.
[56] Sun, J., Gaidai, O., Xing, Y., Wang, F., and Liu, Z., 2023, "On Safe Offshore Energy Exploration in the Gulf of Eilat," Qual. Reliab. Eng. Int., **39**(7), pp. 2957–2966.

[57] Gaidai, O., Xu, J., Yakimov, V., and Wang, F., 2023, "Liquid Carbon Storage Tanker Disaster Resilience," Environ. Syst. Decis., **43**(4), pp. 746–757.
[58] Yakimov, V., Gaidai, O., Wang, F., Xu, X., Niu, Y., and Wang, K., 2023, "Fatigue Assessment for FPSO Hawsers," Int. J. Nav. Archit. Ocean Eng., **15**, p. 100540.
[59] Yakimov, V., Gaidai, O., Wang, F., and Wang, K., 2023, "Arctic Naval launch and Recovery Operations, Under Ice Impact Interactions," Appl. Eng. Sci., **15**, p. 100146.
[60] Gaidai, O., Yakimov, V., Wang, F., Hu, Q., and Storhaug, G., 2023, "Lifetime Assessment for Container Vessels," Appl. Ocean Res., **139**, p. 103708.
[61] Gaidai, O., Xu, J., Yakimov, V., and Wang, F., 2023, "Analytical and Computational Modeling for Multi-Degree of Freedom Systems: Estimating the Likelihood of an FOWT Structural Failure," J. Mar. Sci. Eng., **11**(6), p. 1237.
[62] Gaidai, O., Wang, F., Yakimov, V., Sun, J., and Balakrishna, R., 2023, "Lifetime Assessment for Riser Systems," GRN Tech. Res. Sustainable, **3**(1), p. 4.
[63] Gaidai, O., Yakimov, V., and Zhang, F., 2023, "COVID-19 Spatio-Temporal Forecast in England," Biosystems, **233**, p. 105035.
[64] Gaidai, O., Liu, Z., Wang, K., and Bai, X., 2023, "Current COVID-19 Epidemic Risks in Brazil," Epidemiol. Int. J., **7**(2), pp. 1–10.
[65] Gaidai, O., Yakimov, V., and Balakrishna, R., 2023, "Dementia Death Rates Prediction," BMC Psychiatry, **23**(1), p. 691.
[66] Gaidai, O., Yakimov, V., Wang, F., Zhang, F., and Balakrishna, R., 2023, "Floating Wind Turbines Structural Details Fatigue Life Assessment," Sci. Rep., **13**(1), p. 16312.
[67] Gaidai, O., Yakimov, V., Wang, F., and Zhang, F., 2023, "Safety Design Study for Energy Harvesters," Sustainable Energy Res., **10**(1), p. 15.
[68] Gaidai, O., Yakimov, V., and van Loon, E., 2023, "Influenza-Type Epidemic Risks by Spatio-Temporal Gaidai-Yakimov Method," Dialogues Health, **3**, p. 100157.
[69] Gaidai, O., Yakimov, V., Niu, Y., and Liu, Z., 2023, "Gaidai-Yakimov Reliability Method for High-Dimensional Spatio-Temporal Biosystems," Biosystems **235**, p. 105073.
[70] Gaidai, O., Yakimov, V., Sun, J., and van Loon, E. J., 2023, "Singapore COVID-19 Data Cross-Validation by the Gaidai Reliability Method," npj Viruses, **1**(1), p. 9.
[71] Sun, J., Gaidai, O., Wang, F., and Yakimov, V., 2023, "Gaidai Reliability Method for Fixed Offshore Structures," J Braz. Soc. Mech. Sci. Eng., **46**(1), p. 27.
[72] Gaidai, O., Wang, F., Cao, Y., Liu, Z., 2024, "4400 TEU Cargo Ship Dynamic Analysis by Gaidai Reliability Method," J. Shipp. Trd., **9**(1), p. 1.
[73] Gaidai, O., Wang, F., and Sun, J., 2024, "Energy Harvester Reliability Study by Gaidai Reliability Method," Clim. Resilience Sustainability, **3**(1), p. e64.
[74] Gaidai, O., Sheng, J., Cao, Y., Zhang, F., Zhu, Y., and Loginov, S., 2024, "Public Health System Sustainability Assessment by Gaidai Hypersurface Approach," Curr. Probl. Cardiol., **49**(3), p. 102391.
[75] Gaidai, O., Yakimov, V., Hu, Q., and Loginov, S., 2024, "Multivariate Risks Assessment for Complex Bio-Systems by Gaidai reliability Method," Syst. Soft Comput., **6**, p. 200074.
[76] Gaidai, O., Yakimov, V., Wang, F., Sun, J., and Wang, K., 2024, "Bivariate Reliability Analysis for Floating Wind Turbines," Int. J. Low-Carbon Technol., **19**, pp. 55–64.
[77] Gaidai, O., Yan, P., Xing, Y., Xu, J., and Wu, Y., 2023, "Gaidai Reliability Method for Long-Term Coronavirus Modelling," F1000 Res., **11**, p. 1282.
[78] Yayık, A., Kutlu, Y., Altan, G., 2019, "Regularized HessELM and Inclined Entropy Measurement for Congestive Heart Failure Prediction", Cornell University. https://arxiv.org/abs/1907.05888
[79] Ishihara, T., and Yamaguchi, A., 2015, "Prediction of the Extreme Windspeed in the Mixed Climate Region by Using Monte Carlo Simulation and Measure-Correlate-Predict Method," Wind Energy, **18**(1), pp. 171–186.
[80] Gaidai, O., Sheng, J., Cao, Y., Zhu, Y., and Loginov, S., 2024, "Generic COVID-19 Epidemic Forecast for Estonia by Gaidai Multivariate Reliability Method," Franklin Open, **6**, p. 100075.
[81] Gaidai, O., Sheng, J., Cao, Y., Zhu, Y., Wang, K., and Liu, Z., 2024, "Limit Hypersurface State of Art Gaidai Risk Assessment Approach for Oil Tankers Arctic Operational Safety'," J. Ocean Eng. Mar. Energ, **10**(2), pp. 351–364.
[82] Gaidai, O., Yakimov, V., Wang, F., and Cao, Y., 2024, "Gaidai Multivariate Risk Assessment Method for Energy Harvester Operational Safety, Given Manufacturing Imperfections," Int. J. Precis. Eng. Manuf., **25**(5), pp. 1011–1025.
[83] Gaidai, O., Sheng, J., Cao, Y., Zhang, F., Zhu, Y., and Liu, Z., 2024, "Gaidai Multivariate Risk Assessment Method for Cargo Ship Dynamics", Urban Plann. Transp. Res., **12**, p. 1.
[84] Gaidai, O., 2024, "Global Health Risks Due to the COVID-19 Epidemic by Gaidai Reliability Method," Sci. Talks, **10**, pp. 100366.
[85] Gaidai, O., Cao, Y., Li, H., Liu, Z., Ashraf, A., Zhu, Y., and Sheng, J., 2024, "Multivariate Gaidai hazard Assessment Method in Combination With Deconvolution Scheme to Predict Extreme Wave Heights," Results Eng., **22**, p. 102326.
[86] Gaidai, O., Sun, J., and Cao, Y., 2024, "FPSO/FLNG Mooring System Evaluation by Gaidai Reliability Method," J. Mar. Sci. Technol., **29**(3), pp. 546–555.
[87] Gaidai, O., Ashraf, A., Cao, Y., et al., 2024, "Lifetime Assessment of Semi-Submersible Wind Turbines by Gaidai Risk Evaluation Method," J Mater. Sci: Mater Eng., **19**(1), p. 2.
[88] Gaidai, O., Cao, Y., Ashraf, A., et al., 2024, "FPSO/LNG Hawser System Lifetime Assessment by Gaidai Multivariate Risk Assessment Method," Energy Inf., **7**(1), p. 51.
[89] Gaidai, O., Cao, Y., Zhu, Y., Zhang, F., Liu, Z., and Wang, K., 2024, "Limit Hypersurface State of the Art Gaidai Multivariate Risk Evaluation Approach for Offshore Jacket," Mech. Based Des. Struct. Mach., pp. 1–16.
[90] Gaidai, O., Sheng, J., Cao, Y., Zhu, Y., and Liu, Z., 2024, "Evaluating Areal Windspeeds and Wave Heights by Gaidai Risk Evaluation Method," Nat. Hazard. Rev., **25**(4), p. 05024010.
[91] Gaidai, O., Li, H., Cao, Y., Ashraf, A., Zhu, Y., and Liu, Z., 2024, "Shuttle Tanker Operational Reliability Study by Gaidai Multivariate Risk Assessment Method, Utilizing Deconvolution Scheme," Transp. Res. Interdiscip. Perspect., **26**, p. 101194.
[92] Gaidai, O., Li, H., Cao, Y., Liu, Z., Zhu, Y., and Sheng, J., 2024, "Wind Turbine Gearbox Reliability Verification by Multivariate Gaidai Reliability Method," Results Eng., **23**, p. 102689.
[93] Gaidai, O., Cao, Y., Wang, F., and Zhu, Y., 2024, "Applying the Multivariate Gaidai Reliability Method in Combination With an Efficient Deconvolution Scheme to Prediction of Extreme Ocean Wave Heights," Mar. Syst. Ocean Technol.
[94] Gaidai, O., Ashraf, A., Cao, Y., Sheng, J., Zhu, Y., and Li, H., 2024, "Panamax Cargo-Vessel Excessive-Roll Dynamics Based on Novel Deconvolution Method," Probabilistic Eng. Mech., **77**, p. 103676.
[95] Gaidai, O., Liu, Z., Cao, Y., Sheng, J., Zhu, Y., and Zhang, F., 2024, "Novel Multivariate Design Concept for Floating Wind Turbines by Gaidai Multivariate Reliability Method and Deconvolution Scheme," J. Low Freq. Noise Vibr. Active Control.
[96] Gaidai, O., Ashraf, A., Cao, Y., Zhu, Y., Sheng, J., Li, H., and Liu, Z., 2024, "Multivariate Ocean Waves Dynamics in North Sea and Norwegian Sea by Gaidai Reliability Method," Energy Rep., **12**, pp. 2346–2355.
[97] Gaidai, O., Ashraf, A., Cao, Y., Sheng, J., and Zhu, Y., 2024, "Ocean Windspeeds Forecast by Gaidai Multivariate Risk Assessment Method, Utilizing Deconvolution Scheme," Results Eng., **23**, p. 102796.
[98] Gaidai, O., Cao, Y., Zhu, Y., Ashraf, A., Liu, Z., and Li, H., 2024, "Future Worldwide Coronavirus Disease 2019 Epidemic Predictions by Gaidai Multivariate Risk Evaluation Method," Anal. Sci. Adv., **5**(7–8), p. e2400027.
[99] Gaidai, O., 2024, "Gaidai Risk Evaluation Method for Lifetime Assessment for Offshore Floating Wind Turbine Gearbox," ASME J. Nondestr. Eval., **8**(2), p. 021005.